New Journal of Physics
An Institute of Physics and Deutsche Physikalische Gesellschaft Journal

Charm and strangeness in nuclear reactions at $\sqrt{s} \leq 19$ GeV

Sonja Kabana
Laboratory for High Energy Physics, University of Bern, Sidlerstrasse 5, 3012 Bern, Switzerland
E-mail: sonja.kabana@cern.ch

New Journal of Physics **3** (2001) 16.1–16.21 (http://www.njp.org/)
Received 30 November 2000
Published 20 August 2001

Abstract. We propose to study J/Ψ production in relation with open charm production in nuclear reactions. It appears that a suppression of the J/Ψ over Drell Yan (DY) ratio has been observed by the CERN experiment NA50 in $\mathrm{Pb}+\mathrm{Pb}$ collisions at $\sqrt{s}=17$ GeV above the initial energy density $\epsilon \sim 2.3$ GeV fm^{-3}, which was not seen in $\mathrm{S}+\mathrm{U}$ collisions at $\sqrt{s}=19$ GeV at any ϵ. In our view a clear interpretation of these results has not been achieved. The same experiment has measured an excess in $\mu^+\mu^-$, which can be interpreted as resulting from $D\overline{D}$ decay. We demonstrate that the suppression of the J/Ψ does appear in $\mathrm{S}+\mathrm{U}$ collisions, as well as in $\mathrm{Pb}+\mathrm{Pb}$ collisions at a lower $\epsilon \sim 1$ GeV fm^{-3}, if the J/Ψ is normalized to $D\overline{D}$, instead of DY. This underlines the importance of direct open charm measurements for the interpretation of charmonia suppression. Furthermore we study the dependence of the J/Ψ and $D\overline{D}$ on the number of participating nucleons (N_p). The results indicate non-thermal charm production as expected, and J/Ψ dissociation which is stronger than the absorption seen in other hadrons. We find that the J/Ψ in central $\mathrm{Pb}+\mathrm{Pb}$ collisions is compatible with dominant production from $c\bar{c}$ pair coalescence out of a hadronizing quark and gluon environment. A significant change in the $(J/\Psi)/D\overline{D}$ ratio as well as in the number density of kaons is observed simultaneously above the initial energy density $\epsilon \sim 1$ GeV fm^{-3}, suggesting a change of phase associated with this ϵ.

1. Introduction

Quantum chromodynamics (QCD) on the lattice predicts a phase transition of confined hadronic matter into deconfined quark and gluon matter (called the quark gluon plasma (QGP) state) at a critical temperature $T_c \sim 175$ MeV, respectively at an energy density $\epsilon_c \sim 1$ GeV fm^{-3} [1]. The order of the transition is parameter dependent [2]. An investigation of relevant observables

1367-2630/01/000016+21$30.00

in heavy ion collisions [3] as a function of energy and/or the impact parameter of the collision could/should reveal this transition, through a discontinuous behaviour of many QGP signatures at the transition point.

An anomalous suppression of J/Ψ meson production predicted to be a signature of QGP formation [4] has been measured to occur in the ratio of the J/Ψ over the Drell Yan (DY) process in $\mathrm{Pb}+\mathrm{Pb}$ collisions at $\sqrt{s} = 17$ GeV investigated as a function of transverse energy (E_T) [5]. In $\mathrm{S}+\mathrm{U}$ collisions at $\sqrt{s} = 19$ GeV and in the most peripheral $\mathrm{Pb}+\mathrm{Pb}$ collisions, the $(J/\Psi)/DY$ ratio agrees with expectations [5]. The ratio $(J/\Psi)/DY$ is relevant for the investigation of the J/Ψ suppression, under the assumption that J/Ψ production in these collisions is a hard process.

Recent measurements of the dimuon invariant mass $m(\mu^+\mu^-)$ spectrum between the ϕ and the J/Ψ mass (intermediate mass region (IMR)) revealed a dimuon enhancement above expectation, which increases with the number of nucleons participating in the collision (N_p) [6]. This enhancement can be understood as due to an excess of $D\overline{D}$ production† as suggested by several features of the data, e.g. the shape of the mass, rapidity and transverse momentum distributions of the dimuons [6]. The interpretation of the IMR enhancement as due to open charm is not unique though, because the open charm was extracted through a fit to the dimuon continuum and the $D\overline{D}$ meson signal was not directly identified. Recent work suggesting that the enhancement seen could be due to rescattering of D mesons in nuclear matter [7] is not supported by the data [8]. Another possible interpretation is that the IMR excess could be due to thermal dimuons [9].

Non-perturbative effects are known to play a role in heavy flavour hadron production in elementary reactions, showing up in deviations of data from perturbative QCD calculations [10]. Based on this fact, one could expect that theoretical investigation of non-perturbative effects and different reaction dynamics as in the plasma phase may result in an enhancement of open charm production in nuclear reactions over perturbative QCD expectations.

If the total charm produced in heavy ion collisions indeed deviates from the perturbative QCD expectations for a hard process as suggested by the NA50 data, it follows that the $(J/\Psi)/DY$ ratio is not the proper quantity for the search for J/Ψ suppression as signature of QGP formation in nuclear reactions. It is only the ratio $(J/\Psi)/(\mathrm{total}\ c\bar{c})$ that matters. We therefore investigate here first the dependence of the J/Ψ and the $D\overline{D}$ yields per collision on N_p. We further investigate the dependence of the $(J/\Psi)/D\overline{D}$ ratio on N_p and on the length of the nuclear matter traversed by the J/Ψ, as well as the dependence of both charm and strangeness production on the initial energy density reached in the collision.

2. N_p dependence of charm yields in S + U, Pb + Pb collisions at $\sqrt{s}$ =19, 17 GeV

2.1. N_p dependence of the DY yield

The NA50 collaboration measured the DY yield per nucleus–nucleus collision, produced in $\mathrm{Pb}+\mathrm{Pb}$ collisions at $\sqrt{s} = 17$ GeV per $\mathrm{N}+\mathrm{N}$ pair in arbitrary units, as a function of the transverse energy of the collision (figure 7 in [11]). In this figure it is shown that the theoretically expected DY yield, assuming DY production is a hard process, does partly reproduce the measured one; the deviations at low transverse energy could be understood to result from properties of the lead (Pb) nucleus, in particular from the different radii of the proton and neutron distributions in Pb [12]. It is therefore justified to use the theoretically calculated E_T dependence of DY yield

† By '$D\overline{D}$' we denote the number of D and $\overline{D}$ hadrons which were simultaneously found within the acceptance of the NA50 experiment ($D\overline{D} = (D + \overline{D})_{acc}/2$).

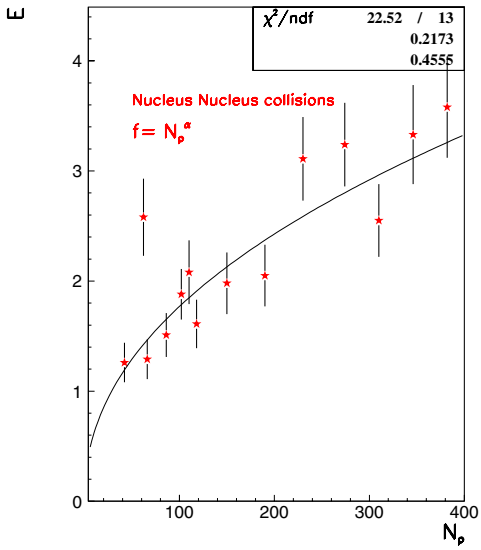

Figure 1. The enhancement E of the open charm yield needed to describe the measured IMR data, as a function of the number of participants. The data are from figure 12 in [6]. The line shows the result of fitting the function $f = cN_p^{\alpha}$. See text for the fit results.

per collision, to estimate the dependence of J/Ψ and $D\overline{D}$ yields on the number of participating nucleons in the collision.

2.2. N_p dependence of the $D\overline{D}$ yield

The NA50 collaboration observed an excess (E) of the measured over the expected $D\overline{D}/DY$ ratio in S + U and Pb + Pb collisions at $\sqrt{s} = 19$, 17 GeV, which increases with the number of participants N_p (figure 12 and table 4 in [6]). If we fit the S + U and Pb + Pb E values of the figure quoted above to a function $f = c \cdot N_p^{\alpha}$, we find that the excess increases with N_p as $N_p^{(\alpha=0.45\pm0.11)}$ (χ^2/degrees of freedom $(DOF) = 1.7$, $DOF = 13$). The data and the fit are shown in figure 1.

The N_p dependence of the excess E of the $D\overline{D}/DY$ production in S + U collisions at $\sqrt{s} = 19$ GeV and Pb + Pb collisions at $\sqrt{s} = 17$ GeV over expectations reflects the N_p dependence of the $D\overline{D}/DY$ ratio. This results from the fact that all other quantities involved in the definition of E [6, 8] do not depend on N_p. Therefore the N_p dependence of the $D\overline{D}$ production yield is given by the N_p dependence of the quantity

$$n_{D\overline{D}} = E \cdot n_{DY} \tag{1}$$

where $n_{D\overline{D}}$, n_{DY} denote the yields of $D\overline{D}$ and DY per collision in arbitrary units. The arbitrary units are due to the fact that NA50 did not publish absolute yields per collision of the J/Ψ, DY and $D\overline{D}$ separately, corrected for losses due to e.g. acceptance, as a function of N_p, E_T. We suggest that it would be important to do so. In short, $n_{D\overline{D}}$ has the same N_p dependence as $(D\overline{D}/DY) \cdot n_{DY}$.

The DY yield used for the above calculation has been extracted from the theoretical curve shown in figure 7 in [11], at the transverse energy (E_T) points in which the $D\overline{D}$ excess factor E has been measured.

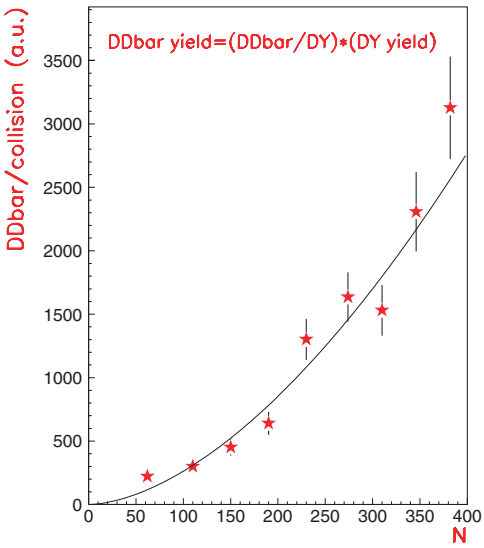

Figure 2. $D\overline{D}$ yield per collision in arbitrary units in $\mathrm{Pb} + \mathrm{Pb}$ collisions at 158 A GeV, as a function of the number of participating nucleons N_p. The line shows the result of fitting the function $f = cN_p^{\alpha}$. See text for the fit results.

We found the E_T points corresponding to the excess factor E by interpolating between the E_T values as a function of the mean impact parameter (b), given in table 1 of [11], to those values of mean impact parameter, at which the factor E has been measured (listed in table 1 of [6]). For the most central and the most peripheral points, for which no mean b are given in table 1 of [6], we estimated the values of b from the dependence of N_p on b calculated for $\mathrm{Pb} + \mathrm{Pb}$ collisions by Ollitrault [13, 14]. These calculations [13] agree with the values (N_p, b) estimated by NA50, when compared in their common range.

The resulting $D\overline{D}$ yield in arbitrary units is shown in figure 2. It increases as $N_p^{(\alpha=1.70\pm0.12)}$ ($\chi^2/DOF = 2.5$, $DOF = 7$). This N_p behaviour indicates that $D\overline{D}$ production in $\mathrm{Pb} + \mathrm{Pb}$ collisions at $\sqrt{s} = 17$ GeV has not yet established equilibrium. If equilibrium would be established, a proportionality with N_p—assuming N_p to be proportional to the volume of the source†—is expected ($\alpha = 1$).

The evidence that $D\overline{D}$ is not yet thermalized, as demonstrated in figure 2, is further justified because the temperature in the collision zone—assuming local thermalization of light particles—is expected to be of the order $\sim 10^2$ MeV, which is much lower than the mass of charm quarks and/or charmed hadrons.

2.3. N_p dependence of the J/Ψ yield

In the following we estimate the J/Ψ yield per collision as a function of N_p, at the same N_p values where the $D\overline{D}$ production was measured. The N_p dependence of the J/Ψ yield per collision is given by the N_p dependence of the quantity

$$n_{J/\Psi} = \frac{J/\Psi}{DY} \cdot n_{DY} \tag{2}$$

† The assumption $N_p \sim V$ is based on the observation that the freeze-out volume V of the particle source is found to be proportional to N_p [15].

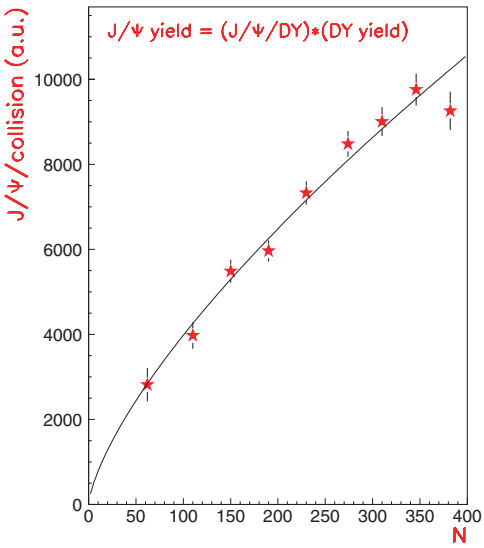

Figure 3. J/Ψ yield per collision in arbitrary units in $\mathrm{Pb}+\mathrm{Pb}$ collisions at 158 A GeV, as a function of the number of participating nucleons N_p. The line shows the result of fitting the function $f = cN_p^{\alpha}$. See text for the fit results.

where $n_{J/\Psi}$, n_{DY} denote the yields of J/Ψ and DY in arbitrary units. The $(J/\Psi)/DY$ values have been extracted from figure 4 of [5] at the E_T values where the E factor has been measured, interpolating between the different points.

The resulting J/Ψ yield per collision produced in $\mathrm{Pb}+\mathrm{Pb}$ collisions in arbitrary units (figure 3) increases like $N_p^{(\alpha=0.70\pm0.04)}$ ($\chi^2/DOF = 1.43$, $DOF = 7$). This N_p dependence indicates an increasing J/Ψ dissociation with higher centrality. The strength of this dissociation as measured by the α parameter is higher for the J/Ψ as compared to any other hadron† produced in these collisions, for example as compared to antiprotons. For the latter, a large annihilation cross section with baryons is expected and there is indeed experimental evidence that they are absorbed with increasing centrality in $\mathrm{Pb}+\mathrm{Pb}$ collisions ($\alpha(\overline{p}) = 0.80 \pm 0.04$ ($\chi^2/DOF = 1.0$, $DOF = 3$) at $y = 3.7$, $p_T = 0$ [15]‡).

The J/Ψ multiplicity as a function of N_p extracted with another method [17] agrees with the results presented here within the errors.

3. The $(J/\Psi)/D\overline{D}$ ratio in nuclear collisions

3.1. The N_p dependence of the $(J/\Psi)/D\overline{D}$ ratio in nuclear collisions

Assuming that the IMR excess is due to open charm allows us to search for an anomalous suppression of J/Ψ as compared to the open charm production. The N_p dependence of the $(J/\Psi)/D\overline{D}$ ratio in $\mathrm{Pb}+\mathrm{Pb}$ and $\mathrm{S}+\mathrm{U}$ collisions at $\sqrt{s}$ of 17 and 19 GeV, estimated as:

$$\frac{J/\Psi}{D\overline{D}} = \frac{(J/\Psi)/DY}{D\overline{D}/DY} \propto \frac{(J/\Psi)/DY}{E} \tag{3}$$

† Deuterons have an even smaller α parameter, but they are not elementary hadrons and are weakly bound (see the discussion in [15]).

‡ We extracted here the α parameter for $\overline{p}$, after quadratically adding the statistical and a 5% systematic error.

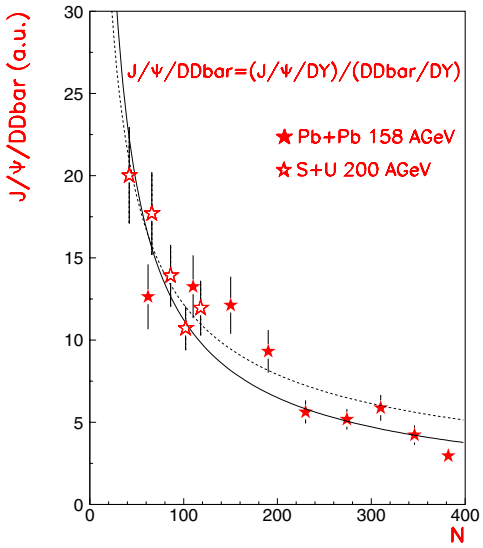

Figure 4. Ratio of J/Ψ to $D\overline{D}$ in arbitrary units in $\mathrm{Pb} + \mathrm{Pb}$ collisions at 158 A GeV (full points) and in $\mathrm{S} + \mathrm{U}$ collisions at 200 A GeV (open points), as a function of the number of participating nucleons N_p. The lines show the result of fitting the function $f = cN_p^{\alpha}$ to the $\mathrm{S} + \mathrm{U}$ (dotted line) and to the $\mathrm{Pb} + \mathrm{Pb}$ data points (full line). See text for the fit results.

in arbitrary units due to the E factor in equation (3), is a decreasing function of N_p (figure 4). The $(J/\Psi)/DY$ in $\mathrm{S} + \mathrm{U}$ collisions was taken from [18, 19].

However NA50 estimated the DY in a different way in the two ratios $(J/\Psi)/DY$ and $D\overline{D}/DY$, which are used in equation (3). Therefore possible deviations of the DY yield from its theoretical calculation (as seen in figure 7 in [11]) do not drop out in the $((J/\Psi)/DY)/(D\overline{D}/DY)$ ratio shown here, because the $D\overline{D}/DY$—unlike the $(J/\Psi)/DY$—was calculated by NA50 not using the minimum bias theoretical DY yield values but the measured ones.

In order to smooth statistical oscillations coming from the pattern of transverse energy versus N_p, the $(J/\Psi)/DY$ ratio divided by $N_p^{0.45\pm0.11}$ is plotted as a function of N_p in figure 5. This quantity resembles the $(J/\Psi)/D\overline{D}$ ratio

$$\frac{J/\Psi}{D\overline{D}} \propto \frac{(J/\Psi)/DY}{N_p^{0.45\pm0.11}} \tag{4}$$

in arbitrary units. The reason is that $N_p^{0.45\pm0.11}$ is the N_p dependence of the $D\overline{D}/DY$ ratio which is illustrated in figure 1:

$$E \propto \frac{D\overline{D}}{DY} \propto N_p^{0.45\pm0.11}.$$

Here we use the results of the fit to the data points of figure 1, instead of the points themselves. The gain is that we can now estimate the $(J/\Psi)/D\overline{D}$ ratio for more points than the nine bins measured in figure 1, as the $(J/\Psi)/DY$ ratio has been measured in more E_T bins than the IMR dimuons, possibly due to the lower statistics available for the latter as seen by the errors.

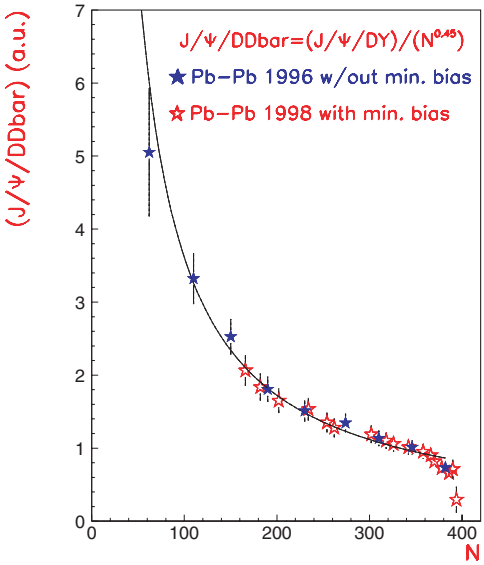

Figure 5. Ratio of $(J/\Psi)/DY$ to $N_p^{0.45\pm0.11}$ in $\mathrm{Pb}+\mathrm{Pb}$ collisions at 158 A GeV as a function of the number of participating nucleons N_p. The nine full star points correspond to the N_p values at which the $D\overline{D}$ yield was measured. The lines show the result of fitting the function $f = cN_p^{\alpha}$ to the full stars. See text for the fit results.

The open points of figure 5 are extracted from the 'minimum bias analysis' results of figure 4 in [5]†. The full points show the quantity $((J/\Psi)/DY)/N_p^{0.45}$ calculated here at the N_p values where the $D\overline{D}$ excess factor was measured.

According to equation (3), the $(J/\Psi)/D\overline{D}$ ratio in $\mathrm{Pb}+\mathrm{Pb}$ collisions, decreases with N_p as $N_p^{(\alpha=-0.79\pm0.14)}$ ($\chi^2/DOF = 3.3$, $DOF = 7$), respectively like $N_p^{(\alpha=-1.17\pm0.14)}$ ($\chi^2/DOF = 1.54$, $DOF = 6$) when the first point is not fitted‡.

The $(J/\Psi)/D\overline{D}$ ratio in S + U collisions (figure 4) decreases with N_p as $N_p^{(\alpha=-0.62\pm0.22)}$ ($\chi^2/DOF = 0.69$, $DOF = 3$).

According to equation (4) the $(J/\Psi)/D\overline{D}$ when fitted to the function N_p^{α} until $N_p = 380$ gives $N_p^{(\alpha=-1.07\pm0.07)}$ ($\chi^2/DOF = 0.93$, $DOF = 7$).

3.1.1. J/Ψ production through coalescence of $c\bar{c}$ quarks. If the J/Ψ is completely dissociated in a quark gluon plasma and is formed later mainly through c and $\bar{c}$ quark coalescence, we expect that the N_p dependence of the ratio $(J/\Psi)/D\overline{D}$—rather than the $(J/\Psi)/(D\overline{D})^2$—reflects the N_p dependence of the volume of the charm environment [10]. This is due to the expectation that, because of the very low cross section of charm production at these energies, there is most often just one $c\bar{c}$ pair per event containing charm, whatever N_p. Then the probability to form a J/Ψ from coalescence is proportional to $(J/\Psi)/D\overline{D}$ and inversely proportional to the volume

† 'Minimum bias analysis' in NA50 means that the DY for the $(J/\Psi)/DY$ ratio was determined using the theoretically estimated DY yield per collision as a function of E_T and the measured $\mathrm{d}N/\mathrm{d}E_T$ versus E_T spectrum of minimum bias trigger events (see [11]).

‡ The first point of the $D\overline{D}/DY$ enhancement factor E lies significantly above the N_p^{α} function fit to the E distribution (figure 12 in [6]).

of the particle source—made up by $u\bar{u}d\bar{d}s\bar{s}$ quarks and gluons—within which the c and $\bar{c}$ quarks scatter. Assuming this volume is proportional to N_p (see the footnote on p 16.4), one would expect that $(J/\Psi)/D\overline{D}$ decreases as N_p^{-1}, as actually derived here.

In this case, one can use the $(J/\Psi)/D\overline{D}$ ratio to extract the absolute value of the volume of its environment with a coalescence model. The 'charm' coalescence volume would reflect partly the QGP hot spot volume and partly the hadronic source volume from which hadrons with charm and anticharm can also form a J/Ψ. If the absolute yields per collision of J/Ψ and $D\overline{D}$ as a function of N_p needed for this calculation were published by NA50, the charm coalescence volume could be calculated. In the next section we give an approximate estimate of this volume.

Figure 5 suggests that the coalescence picture could hold for the full N_p range of $\mathrm{Pb}+\mathrm{Pb}$ collisions up to $N_p = 380$†. Indeed the results of the $f = cN_p^{\alpha}$ fit to data of figure 5 show that the $J/\Psi/D\overline{D}$ ratio decreases proportionally to $1/N_p$. This dependence as discussed above is the one expected if J/Ψ forms out of coalescence of $c\bar{c}$ quarks.

On the other hand, if the multiplicity of charm quarks is high enough that often more than one charm quark pair per event with charm is produced, then it is the ratio $(J/\Psi)/(D\overline{D})^2$ which is expected to be inversely proportional to the volume of the charm source (this is exactly the case if d coalescence out of p and n is investigated in a baryon-rich source). The N_p dependence of the $(J/\Psi)/(D\overline{D})^2$ ratio, which would be relevant in the above discussed case, is $N_p^{(\alpha=-2.26\pm0.48)}$ ($\chi^2/DOF = 2.5$, $DOF = 7$) respectively $N_p^{(\alpha=-3.1\pm0.24)}$ ($\chi^2/DOF = 1.2$, $DOF = 6$) if the first point is not fitted. The question on the absolute multiplicity of charm in nuclear reactions should be answered by experiment.

3.1.2. An estimate of the size of the charm source. In the following we give an estimate of the volume of the charm source in central $\mathrm{Pb}+\mathrm{Pb}$ collisions. We first estimate the $J/\Psi/D\overline{D}$ ratio in absolute units, using the following information. We take the cross section for $c\bar{c}$ production in $\mathrm{p}+\mathrm{p}$ collisions at 200 GeV per nucleon from [20, 21]:

$$\sigma(\mathrm{pp} \to c\bar{c}) = 5\mu\mathrm{b}$$

and the cross section for J/Ψ production in the same reactions from [20, 22]:

$$\sigma(\mathrm{pp} \to J/\Psi) = 143\ \mathrm{nb}.$$

Therefore the ratio of J/Ψ to total $c\bar{c}$ production in $\mathrm{p}+\mathrm{p}$ collisions at 200 GeV per nucleon is

$$\frac{J/\Psi}{c\bar{c}} = 0.0286.$$

However, the expectation value of the $(J/\Psi)/D\overline{D}$ in central $\mathrm{Pb}+\mathrm{Pb}$ collisions is lower as compared to $\mathrm{p}+\mathrm{p}$ collisions, due to absorbtion of the J/Ψ. This is indicated by the curve in figure 6, which represents the expectation for the $(J/\Psi)/DY$ ratio as a function of the path L of J/Ψ through nuclear matter‡. The expectation value of the $(J/\Psi)/DY$ ratio for the central $\mathrm{Pb}+\mathrm{Pb}$ data (very last point, at the highest L value) is smaller by a factor 2.8 as compared to the expectation for the $\mathrm{p}+\mathrm{p}$ collisions (first point, at the lowest L value).

† Obviously, it would be better to use the $D\overline{D}$ data themselves instead of the N_p parametrization if high enough statistics were available.

‡ The $J/\Psi/DY$ and the $(J/\Psi)/D\overline{D}$ ratios expected from $\mathrm{p}+\mathrm{p}$ collisions both have the same L dependence.

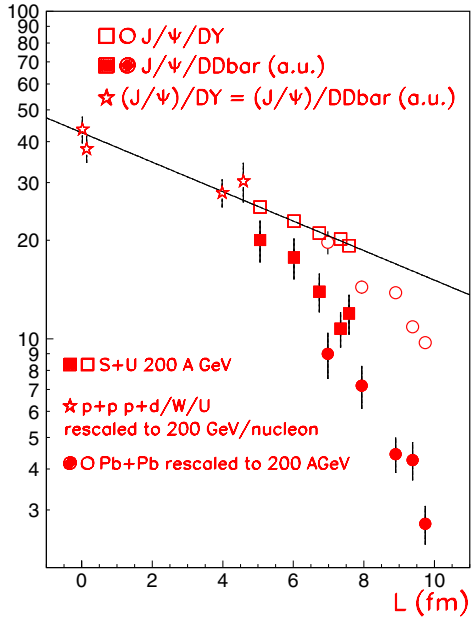

Figure 6. The open points show the ratio of J/Ψ to DY in $\mathrm{p}+\mathrm{A}$, $\mathrm{S}+\mathrm{U}$ and $\mathrm{Pb}+\mathrm{Pb}$ collisions normalized to 200 A GeV, as a function of the path of J/Ψ through nuclear matter L [18, 19]. The full points show the ratio of J/Ψ to $D\overline{D}$ in $\mathrm{S}+\mathrm{U}$ and $\mathrm{Pb}+\mathrm{Pb}$ collisions at 200 A GeV estimated here. The open stars show the L dependence of the $(J/\Psi)/DY$ and the $(J/\Psi)/D\overline{D}$ ratio in $\mathrm{p}+\mathrm{A}$ collisions. All $(J/\Psi)/D\overline{D}$ ratios shown in this figure are in arbitrary units.

We therefore correct the above found value for $(J/\Psi)/c\bar{c} = 0.0286$, by the factor 2.8 and arrive at an approximate estimate for the ratio $(J/\Psi)/c\bar{c}$ in central $\mathrm{Pb}+\mathrm{Pb}$ collisions of

$$\frac{J/\Psi}{c\bar{c}}(\text{expected, central Pb} + \text{Pb}) = 0.0102.$$

The measured over the expected $(J/\Psi)/D\overline{D}$ ratio, for central $\mathrm{Pb}+\mathrm{Pb}$ events from figure 9(a) (second point from the end), is

$$\frac{J/\Psi}{D\overline{D}}(\text{measured/expected, central Pb} + \text{Pb}) = 0.145.$$

We assume that

$$\frac{(J/\Psi)/D\overline{D}(\text{measured, central Pb} + \text{Pb})}{(J/\Psi)/D\overline{D}(\text{expected, central Pb} + \text{Pb})} \sim \frac{(J/\Psi)/c\bar{c}(\text{measured, central Pb} + \text{Pb})}{(J/\Psi)/c\bar{c}(\text{expected, central Pb} + \text{Pb})}.$$

Finally we estimate the measured $(J/\Psi)/c\bar{c}$ in absolute units as follows:

$$\begin{aligned}\frac{J/\Psi}{c\bar{c}}&(\text{measured, abs. units, central Pb} + \text{Pb}) \\ &\sim \frac{(J/\Psi)/c\bar{c}(\text{measured, central Pb} + \text{Pb})}{(J/\Psi)/c\bar{c}(\text{expected, central Pb} + \text{Pb})} \cdot \frac{J/\Psi}{c\bar{c}}(\text{expected, central Pb} + \text{Pb}) \\ &= 0.145 \times 0.0102 = 0.004\,15.\end{aligned}$$

We use now this value of $(J/\Psi)/c\bar{c}$ to estimate the volume of the charm source for the most central $\mathrm{Pb}+\mathrm{Pb}$ collisions at 158 A GeV, with the simple Ansatz:

$$\frac{J/\Psi}{c\bar{c}} = \frac{V_{J/\Psi}}{V_{charm\ source}} \rightarrow V_{charm\ source} = \frac{c\bar{c}}{J/\Psi} \cdot V_{J/\Psi}$$

where $V_{J/\Psi}$ is the volume of the J/Ψ and $V_{charm\ source}$ the total volume of the charm source. Assuming that $V_{J/\Psi}$ is equal to $\frac{4}{3}\pi 0.4^3\ \mathrm{fm}^3 = 0.268\ \mathrm{fm}^3$ [23] we find

$$V_{charm\ source} = 64.6\ \mathrm{fm}^3.$$

The radius of this source (assuming a sphere) is $R_{charm\ source} = 2.49$ fm.

We can further compare the above value of the charm source radius with the expectation for the radius of the source of most hadrons (π, K etc) at the thermal freeze-out. For this we have to take into account the decrease of the radius with transverse mass [15]. We estimate this from the parametrization given in [15]:

$$R = 10.4 \cdot (1 + m_T \cdot 9.3)^{-1/2} \qquad (R \text{ in fm}, m_T \text{ in GeV}).$$

This parametrization fits well the radii extracted from $\pi\pi$ correlations measured by NA49, as well as coalescence radii from the d/p^2 ratio measured by NA52 [15], both measured in central $\mathrm{Pb}+\mathrm{Pb}$ collisions at 158 A GeV.

The expected radius of the charm source at transverse mass equal to the mass of the D meson and near zero transverse momentum (1.86 GeV) is $\sim$2.43 fm, which is therefore very similar to the estimation of $R_{charm\ source} \sim 2.49$ fm.

3.2. The L dependence of the $(J/\Psi)/D\overline{D}$ ratio in nuclear collisions

The two distributions of $(J/\Psi)/D\overline{D}$ ratio for $\mathrm{S}+\mathrm{U}$ and $\mathrm{Pb}+\mathrm{Pb}$ collisions in figure 4 are measured at different energies, and therefore they cannot be compared in terms of their absolute yields but only with respect to their shapes. In order to compare their absolute yields, the data from figure 5 of [19] will be used. There the $(J/\Psi)/DY$ ratio in $\mathrm{p}+\mathrm{A}$, $\mathrm{S}+\mathrm{U}$ and $\mathrm{Pb}+\mathrm{Pb}$ collisions is shown as a function of L, all normalized to the same energy ($\sqrt{s} = 19$ GeV) and corrected for the isospin dependence of DY production. The parameter L is the length that the J/Ψ traverses through nuclear matter. In order to convert figure 5 of [19] to the $(J/\Psi)/D\overline{D}$ ratio as a function of the L parameter, the $(J/\Psi)/DY$ ratio data points have been divided by the E factor as described in equation (3). The correlation of the L parameter with N_p and b for $\mathrm{Pb}+\mathrm{Pb}$ collisions has been estimated using the theoretical calculation of [13].

The L dependence of the $(J/\Psi)/D\overline{D}$ ratio in arbitrary units in $\mathrm{p}+\mathrm{A}$, $\mathrm{S}+\mathrm{U}$ and $\mathrm{Pb}+\mathrm{Pb}$ collisions calculated here is shown in figure 6, together with the $(J/\Psi)/DY$ ratio published in [18, 19]. The full points show the $(J/\Psi)/D\overline{D}$ ratio in $\mathrm{S}+\mathrm{U}$ and $\mathrm{Pb}+\mathrm{Pb}$ collisions extracted as indicated in equation (3). The open squares and circles show the $(J/\Psi)/DY$ ratio in $\mathrm{S}+\mathrm{U}$ and $\mathrm{Pb}+\mathrm{Pb}$ collisions from [18, 19]. The open stars show both the L dependence of the $(J/\Psi)/DY$ as well as the L dependence of the $(J/\Psi)/D\overline{D}$ in $\mathrm{p}+\mathrm{A}$ collisions which are the same, since the factor E has the value 1 for the latter.

The J/Ψ over the $D\overline{D}$ production investigated as a function of L (respectively as a function of the volume, since $V \sim L^3$), is suppressed as compared to the shape of the exponential fit going through the $(J/\Psi)/D\overline{D}$ $\mathrm{p}+\mathrm{A}$ data, in both the $\mathrm{S}+\mathrm{U}$ and $\mathrm{Pb}+\mathrm{Pb}$ collisions at all L points (line in figure 6).

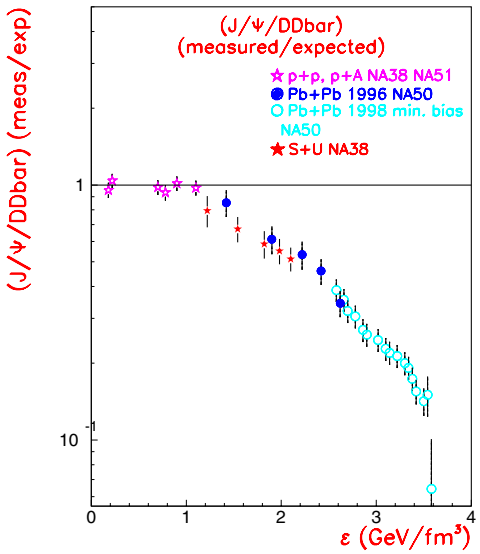

Figure 7. The $(J/\Psi)/D\overline{D}$ (measured/'expected') ratio is shown as a function of the initial energy density (ϵ) achieved in the collisions investigated.

The initial energy density of the lowest $\mathrm{S}+\mathrm{U}$ point has been estimated to be $\sim$1.1 GeV fm^{-3} [5], which is comparable to the predicted critical energy density for the QGP phase transition of $\sim$1 GeV fm^{-3}. A similar energy density of 1.2 GeV fm^{-3} has been estimated [5] to be reached in the most peripheral $\mathrm{Pb}+\mathrm{Pb}$ collisions measured by NA50.

In the following we investigate the initial energy density, rather than only the volume of the particle source ($V \sim L^3$), as a critical parameter for the appearance of the QGP phase transition.

4. The ϵ dependence of charm and strangeness in nuclear collisions

4.1. Charm

We estimate here the $(J/\Psi)/D\overline{D}$ ratio as a function of the initial energy density ϵ. For this purpose we use part of the data shown in figure 7 in [5]. There the ratio of $((J/\Psi)/DY)_{measured}$ over the $((J/\Psi)/DY)_{expected}$ is shown. The '$((J/\Psi)/DY)_{expected}$' is taken to be the exponential fit seen in figure 6, which represents the 'normal' J/Ψ dissociation (i.e. understood without invoking QGP formation). Dividing these data points by $N_p^{0.45\pm0.11}$, and normalizing the distribution of $\mathrm{S}+\mathrm{U}$ and $\mathrm{Pb}+\mathrm{Pb}$ points to the $\mathrm{p}+\mathrm{p}$ and $\mathrm{p}+\mathrm{A}$ data as in figure 6, we estimate the $((J/\Psi)/D\overline{D})$ ratio over the expectation expressed by the above-mentioned exponential curve, which fits the $((J/\Psi)/D\overline{D})$ data points for $\mathrm{p}+\mathrm{p}$, $\mathrm{p}+\mathrm{d}$ and $\mathrm{p}+\mathrm{A}$ collisions.

The result of this calculation is shown in figure 7 on a logarithmic scale and in figure 9(a) on a linear scale. It demonstrates a deviation of the $(J/\Psi)/D\overline{D}$ ratio both in $\mathrm{S}+\mathrm{U}$ and $\mathrm{Pb}+\mathrm{Pb}$ collisions, from the $\mathrm{p}+\mathrm{p}$ and $\mathrm{p}+\mathrm{A}$ expectation curve, occurring above $\epsilon \sim 1$ GeV fm^{-3}. The logarithmic scale is shown to reveal small changes in the slope of the $((J/\Psi)/D\overline{D})$ distribution as a function of ϵ, appearing at $\epsilon \sim 2.2$ and 3.2 GeV fm^{-3}.

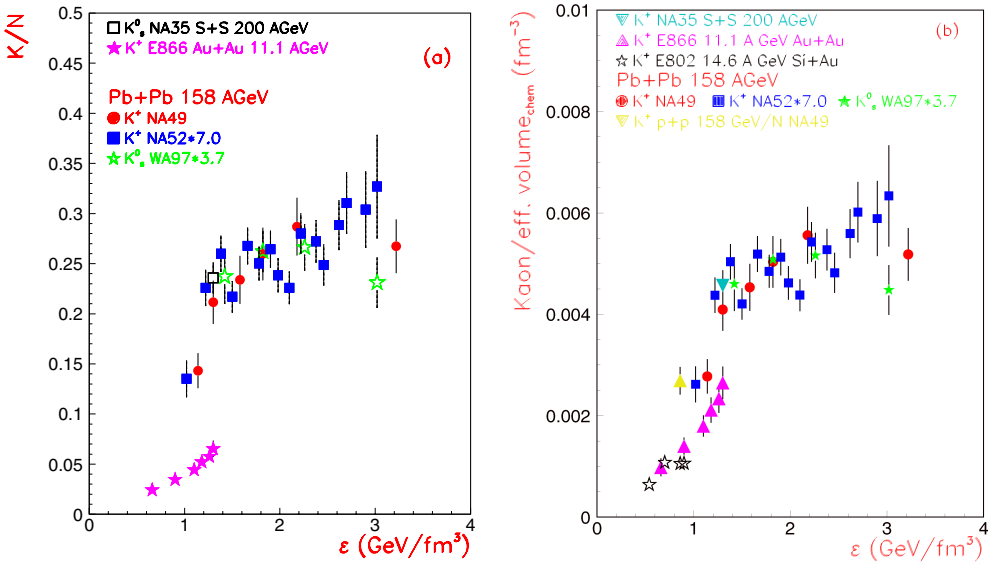

Figure 8. (a) The kaon ($\sim K^+$) multiplicity per participant nucleon is shown as a function of the initial energy density (ϵ). (b) The kaon ($\sim K^+$) multiplicity over the effective volume of the particle source at chemical freeze-out, in the centre of mass frame, is shown as a function of the initial energy density (ϵ). The above effective volume is smaller than the real source volume but proportional to it.

4.2. Strangeness

Figure 8(a) shows the multiplicity of kaons per event (K^+, but also some K^0_s data scaled to K^+, are shown) divided by the number of participating nucleons N_p as a function of the initial energy density (see below for the calculation details). A change in the behaviour of kaons per participant nucleon occurs around $\epsilon \sim 1$ GeV fm^{-3}.

As previously mentioned (see footnote on p 16.4) we assume that the number of participant nucleons is proportional to the volume of the source at freeze-out. However the proportionality factor may be different at different $\sqrt{s}$. We therefore estimate in the following the volume at thermal and chemical freeze-out and investigate the kaon yield per volume as a function of ϵ. The results are shown in figure 8(b) for the chemical freeze-out and in figure 9(b) for the thermal freeze-out (see below for the calculation details).

Figure 9 compares the two QGP signatures of J/Ψ suppression and of strangeness enhancement. For this purpose we represent all data points as a function of the estimated energy density. Note that the energy density as critical scale variable has the advantage that, unlike the temperature, it is defined irrespective of whether equilibrium is reached in the collisions studied.

Figure 9(b) shows the multiplicity of kaons per event (K^+, but also some K^0_s data scaled to K^+, are shown) divided by the effective volume of the particle source at thermal freeze-out in the centre of mass frame, as a function of the initial energy density. The effective volume represents the part of the real source volume, within which pions are correlated with each other (called 'homogeneity' volume in the literature [24]). The effective volume is smaller than but proportional to the real source volume. For a more precise calculation of the freeze-out source

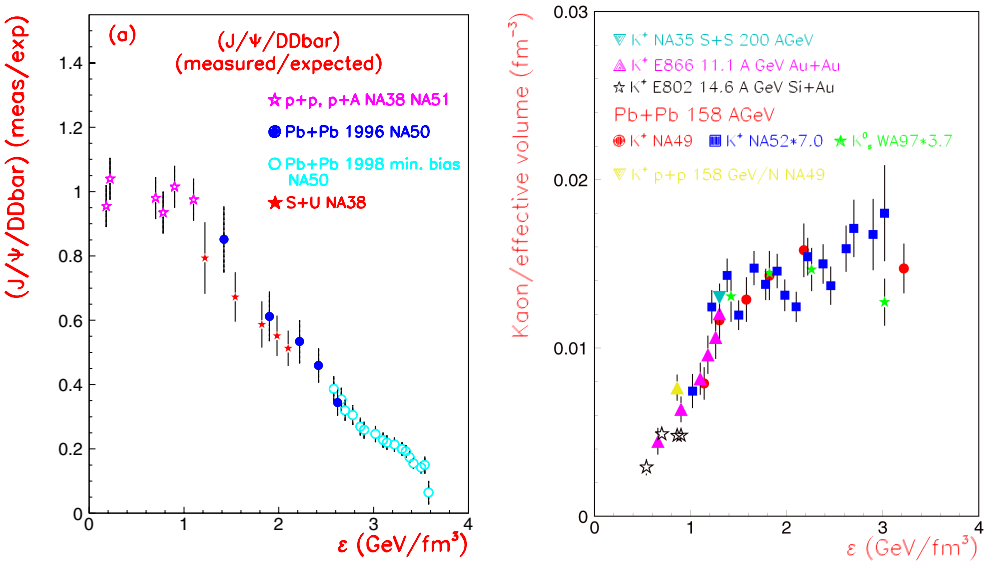

Figure 9. (a) The $(J/\Psi)/D\overline{D}$ (measured/'expected') ratio is shown as a function of the initial energy density (ϵ) achieved in the collisions investigated. (b) The kaon ($\sim K^+$) multiplicity over the effective volume ($V = (\pi \cdot 4 \cdot R^2_{side}) \cdot (\sqrt{12} \cdot R_{long})$) of the particle source at thermal freeze-out, in the centre of mass frame, is shown as a function of the initial energy density (ϵ). The above effective volume is smaller than the real source volume but proportional to it.

volume a detailed model is needed. Here we estimate the effective volume at thermal freeze-out $V_{thermal}$ based on measurements. The (smaller) effective volume at chemical freeze-out $V_{chemical}$ is not experimentally measured, we give however an estimate.

Note that we compare the kaon data without rescaling for the different energy between Alternating Gradient Synchrotron (AGS) and Super Proton Synchrotron (SPS)†. The reason for this omission is the following: kaons due to their small mass can be produced easily in secondary and tertiary interactions of initial nucleons or of secondary produced particles (π), in contrast to charm at SPS energy which is mainly produced in the first interaction. Because of this, the rescaling of kaons produced in $\mathrm{A} + \mathrm{A}$ collisions at different energies using kaon production in $\mathrm{p} + \mathrm{p}$ collisions is only approximately right, as the secondary and tertiary collisions occur at a smaller effective $\sqrt{s}$. It would be exactly right if kaon production were only the result of first collisions occurring at the nominal $\sqrt{s}$ of the projectiles. Furthermore, figures 8(b) and 9(b) do not compare the expected with the measured kaon yield, but the kaon number density itself, at different $\sqrt{s}$.

4.2.1. Estimation of the source volume at thermal freeze-out. The effective volume V of the particle source has been estimated in the centre of mass frame, assuming a cylindrical shape of the source:

$$V = (\pi \cdot Radius^2_{cylinder}) \cdot Length_{cylinder} = (\pi \cdot 4 \cdot R^2_{side}) \cdot (\sqrt{12} \cdot R_{long})$$

† The total K^+ multiplicity in $\mathrm{p} + \mathrm{p}$ collisions increases by a factor of $\sim$5, from 11.1 to 158 GeV per nucleon [25].

where R_{side} is a measure of the transverse radius and R_{long} is a measure of the longitudinal radius of the particle source, and the factors 4 and $\sqrt{12}$ arise from the definition of R_{side}, R_{long} [24]. The R_{side} and R_{long} values for central $\mathrm{Au}+\mathrm{Au}$ collisions at 10.8 A GeV and for central $\mathrm{Pb}+\mathrm{Pb}$ collisions at 158 A GeV have been taken from [26]. We haven't used the more elaborated estimation of the homogeneity volume given in [27], because the R_{ol} component is not given in [26]. For the definitions of the radii R_{side}, R_{long} and R_{ol} see [27]. Based on the data of [26] we estimated the effective volume of the source at thermal freeze-out in central $\mathrm{Au}+\mathrm{Au}$ collisions at 10.8 A GeV ($V \sim 1949\ \mathrm{fm}^3$) and central $\mathrm{Pb}+\mathrm{Pb}$ collisions at 158 A GeV ($V \sim 6532\ \mathrm{fm}^3$). The effective volume increases by a factor of 3.35 from AGS to SPS energy.

The ratio K/N_p is expected to be proportional to the number density of kaons $\sim K/V$, (V = volume), assuming $V \sim N_p$ (for justification of this assumption see † on p 1.4, [26] and [30]). Based on this expectation, we estimated here the K/V ratios from the K/N_p ratios, by normalizing the K/N_p ratios to the K/V value of the most central $\mathrm{Au}+\mathrm{Au}$ events of E866, respectively $\mathrm{Pb}+\mathrm{Pb}$ events of NA49, for which the value of the volume has been estimated above.

The kaon data from Au+Au collisions at 11.1 A GeV (E866 and E802 experiments) [31] and from $\mathrm{Pb}+\mathrm{Pb}$ collisions at 158 A GeV (NA49 experiment) [32] are kaon multiplicities extrapolated to full acceptance. Therefore NA49 and E866 data are absolutely normalized. We estimated K/N_p from the NA49 experiment using the kaon multiplicities from [32] and the number of wounded nucleons from [33] as available†, otherwise we used the N_p estimated from the experimental baryon distribution [32].

The data from NA52 [15, 16] and WA97 [34] have been measured in a small phase space acceptance and have been scaled here arbitrarily, in order to match the NA49 data in figure 9. This scaling is justified since all NA52, NA49 and WA97 measurements are kaons produced in $\mathrm{Pb}+\mathrm{Pb}$ collisions at 158 A GeV, and 'extrapolates' the NA52 and WA97 data to the NA49 full acceptance multiplicities, allowing for comparison of the shapes of the distributions. It is assumed that the N_p and ϵ dependence of kaons does not change significantly with the phase space acceptance.

4.2.2. Estimation of the source volume at chemical freeze-out. Based on the temperature at thermal and chemical freeze-out which has been estimated from measurements using thermal models [28], and the above-estimated volumes at thermal freeze-out, we can further estimate the volume at chemical freeze-out. For this we assume that the relation $V \sim T^{-3}$, which holds in the universe for massless particles in thermal equilibrium and for adiabatic expansion [29], holds approximately for heavy ion collisions at AGS and SPS energy. Then from the temperature values at thermal and chemical freeze-out given in [28] averaged over all models, we find that the ratio $V_{chemical}/V_{thermal}(\mathrm{AGS\ Si}+\mathrm{Au\ 14.6\ A\ GeV}) = 0.45$ and $V_{chemical}/V_{thermal}(\mathrm{SPS\ Pb}+\mathrm{Pb}$ 158 A GeV$) = 0.28$. Using the volume at chemical freeze-out as estimated above would stretch apart the K/V ratio in figure 9(b) between SPS and AGS, by a factor $\sim$1.6. We haven't used these values in figure 9, because the above calculation is model dependent, e.g. the assumption of massless particles is not met, while the assumption of thermal equilibrium may not be true.

Figure 8(b) shows the multiplicity of kaons per event divided by the effective volume of the source at chemical freeze-out, as a function of the initial energy density.

† We take N_p equal to the number of wounded nucleons for NA49, because it is used in all other experiments presented here, and allows for a straightforward geometrical interpretation of N_p.

4.2.3. Estimation of the initial energy density. In order to calculate the energy density we have performed the following steps. The energy density for all colliding systems has been estimated using the Bjorken formula [35] and data given in [31, 36, 37]. The transverse radius of the overlapping region of the colliding nuclei is found as: $R_{trans} = 1.13 \cdot (N_p/2)^{1/3}$, where N_p is the total number of participant nucleons. The formation time was taken to be $1\ \mathrm{fm}/c$ [35].

The E866 experiment did not measure E_T, but instead the forward going energy $E_{forward}$ of the nucleons which did not interact (spectators). Therefore in order to estimate the ϵ for E866 we did the following. We assumed that the transverse energy at midrapidity is proportional to the total energy of the nucleons participating in the collision:

$$(\mathrm{d}E_T/\mathrm{d}\eta)_{ycm} \propto E_{tot,part}$$

and therefore to the number of participant nucleons. In this way, we estimate the $(\mathrm{d}E_T/\mathrm{d}\eta)_{ycm}$ in arbitrary units, from the number of participants and the Bjorken estimate.

In order to normalize properly to the absolute units of energy density, we use one value of ϵ from the literature, namely the energy density in the most central $\mathrm{Au} + \mathrm{Au}$ events at this energy of 1.3 GeV fm^{-3}, given in [36].

We then normalized the results in such a way that the maximum energy density of our estimate matches the absolute value of the maximal achieved energy density in the most central Au+Au events of 1.3 GeV fm^{-3}.

We estimate the N_p dependence of the initial energy density in $\mathrm{Si}+\mathrm{Au}$ collisions at 14.6 GeV per nucleon in the same way [51]. We normalized the results in such a way that the maximum energy density of our estimate matches the absolute value of the maximal achieved energy density in the most central $\mathrm{Si} + \mathrm{Au}$ collisions, which is estimated to be $\sim$0.9 GeV fm^{-3} [50]. See below for an estimate of the systematic error associated with this approximation.

NA52 measures E_T near midrapidity ($y \sim 3.3$). These values were used to estimate the energy density as a function of N_p. However NA52 did not correct the measured E_T value e.g. for the phase space acceptance. For this reason NA52 does not give an estimate of the fully corrected $\mathrm{d}E_T/\mathrm{d}\eta$ near midrapidity. The NA52 E_T results have therefore been normalized to match the maximum energy density reached in $\mathrm{Pb} + \mathrm{Pb}$ collisions of $\epsilon_{max} = 3.2$ GeV fm^{-3}, extracted by NA49 in [37], in events with the same centrality. Parametrizing the dependence of the energy density on the number of participants found from the NA52 data as described above, we estimated the energy density corresponding to the N_p values of the WA97 and the NA49 kaon measurements, given in [32, 34]. Data from $\mathrm{S} + \mathrm{S}$ collisions at 200 GeV per nucleon and $\mathrm{p} + \mathrm{p}$ collisions at 158 GeV per nucleon [51] taken from [32] and [37, 38] are also shown.

To estimate the systematic error on the energy density found with the above methods, we calculated the energy density in $\mathrm{Pb} + \mathrm{Pb}$ collisions at 158 A GeV, using the VENUS 4.12 [39] event generator. We estimated with VENUS the $(\mathrm{d}E_T/\mathrm{d}\eta)_{ycm}$ at $ycm = \mathrm{midrapidity}$ and the number of participant nucleons and used them to find the energy density from the Bjorken formula [35]. The deviation of the energy density calculated with VENUS $(\mathrm{d}E_T/\mathrm{d}\eta)_{ycm}$ from the energy density found using the NA52 transverse energy measurements is $\leq$30% of the latter. The deviation of the energy density calculated with VENUS $\mathrm{d}E_T/\mathrm{d}\eta$ from the energy density found using the total energy of the participant nucleons and of the newly produced particles (which is similar to the method used to estimate the energy density for the AGS data), over the latter energy density, is at the same level.

In this context, it appears important for a more precise comparison of data as a function of ϵ that experiments publish together with the number of participants also the $\mathrm{d}E_T/\mathrm{d}\eta$ at midrapidity

for each centrality region, for both nucleus + nucleus and for p + p collisions, estimated by models or measured if available (e.g. in NA49).

4.3. Comparison of charm and strangeness

Figure 9(b) suggests that kaons below $\epsilon \sim 1$ GeV fm^{-3} did not reach equilibrium, while this seems to be the case above. Indeed kaons produced in Au + Au collisions at 11.1 A GeV [31] and in very peripheral Pb + Pb collisions at 158 A GeV [15, 16, 40, 41] increase faster than linear with N_p, indicating non-thermal kaon production, while they increase nearly proportional to N_p above $\epsilon \sim 1$ GeV fm^{-3} [15, 16, 34, 41]. The connection of strangeness equilibrium and the QGP phase transition has been discussed e.g. in [42]. There it is shown that strangeness in heavy ion collisions is expected to reach equilibrium values if the system runs through a QGP phase, while this is less probable in a purely hadronic system.

Figure 9 demonstrates that both the J/Ψ and kaon production exhibit a dramatic change above the energy density of $\sim$1 GeV fm^{-3}. While the equilibration of strange particles as suggested by their $\sim N_p^1$ dependence above 1 GeV fm^{-3} could in principle also be due to equilibrium reached in a hadronic environment, the combined appearance of this effect and of the $(J/\Psi)/D\overline{D}$ suppression at the same energy density value is a striking result, indicating a change of phase above $\epsilon_c = 1$ GeV fm^{-3}.

The expectation for the shape of the J/Ψ suppression as a function of energy density are three successive drops of the J/Ψ [5, 43]; a drop by $\sim$8% [17] due to ψ' dissociation, a drop by $\sim$32% [17] due to χ_c dissociation and a drop by $\sim$100% due to J/Ψ dissociation. These occur without taking into account regeneration of J/Ψ through other processes. These can be e.g. coalescence of charm quarks or J/Ψ not travelling through the plasma. The ψ' feeds only 8% of the total J/Ψ's and can therefore hardly be observed as a break in the J/Ψ production.

The absolute value of the energy density ϵ and therefore of the N_p values at which these changes could be observed are not exactly given by the models. The critical energy densities for the dissociation of the states Ψ', χ_c and J/Ψ could even be so near to each other that no clear multistep behaviour is seen in $(J/\Psi)/D\overline{D}$. A possible reason for this to happen is that the binding energies of charmonia change once the potential becomes deconfined and come much closer to each other and to the 'ionization' energy. This is also in agreement with the expectations of [54].

Figure 9 suggests that the breaks in the $(J/\Psi)/D\overline{D}$ ratio at $\epsilon \sim 2.2$ and 3.2 GeV fm^{-3}, are less dramatic than the change above $\epsilon \sim 1$ GeV fm^{-3}. Therefore, all bound $c\bar{c}$ states could be dissociated at similar energy densities, which lie near 1 GeV fm^{-3}.

Alternatively, the ψ' and the χ_c could dissociate above $\epsilon \sim 1$ GeV fm^{-3} and the dissociation of the J/Ψ could start at $\epsilon = 2.2$ GeV fm^{-3}, if we interpret the change in the $(J/\Psi)/D\overline{D}$ ratio, below and above $\epsilon = 2.2$ GeV fm^{-3}, as a step behaviour. In this context, the steep drop of the $(J/\Psi)/D\overline{D}$ ratio in the bin(s) of largest N_p (figures 5, 7 and 9) cannot be interpreted in a natural way. The steps of $(J/\Psi)/D\overline{D}$ remain to be established through a direct measurement of J/Ψ and $D\overline{D}$ absolute yields as a function of (E_T, N_p, ϵ).

In the picture discussed above, three QGP signatures appear in nuclear collisions at energy density larger than $\sim$1 GeV fm^{-3}:

(a) J/Ψ suppression (figure 9(a))—which could be due to bound $c\bar{c}$ states dissociation,

(b) enhancement of strangeness density (figure 9(b)),

(c) the invariant mass $m(e^+e^-)$ excess at m below the ρ mass [44], possibly due to a ρ change [45] and/or to increased production of the lowest mass glueball state in QGP [46].

This coincidence of QGP signatures, suggests a change of phase at $\epsilon \sim 1$ GeV fm^{-3} as expected [1].

From the above discussion, it follows that a direct measurement of open charm production in nuclear collisions appears essential for the physics of the QGP phase transition. Furthermore, if enhanced over expectations, open charm in nuclear collisions defies theoretical understanding.

5. Possibilities for future measurements

A measurement of open and closed charm production in Pb+Pb collisions as a function of energy below the SPS top energy of $\sqrt{s} = 17$ GeV, searching for the disappearance of the observed J/Ψ suppression in central Pb + Pb collisions at a certain $\sqrt{s}$, could prove clearly the QGP phase transition. Using the same nuclei at different $\sqrt{s}$ and looking only at central collisions, differences due to different nuclear profiles drop out. No currently existing experiment at SPS is however able to perform this measurement without major upgrades, although one future experiment (NA60) could significantly improve the identification of open charm production through a better determination of the decay vertex [47]. The study could also be performed at the Relativistic Heavy Ion Collider (RHIC) using lower energy and/or large and small nuclei, and in fixed target experiments at RHIC favoured because of higher luminosity as compared to the collider mode, which is important for a low-energy scan.

It would also be important (and easier than the above) to measure the J/Ψ, $D\overline{D}$ and DY absolute yields per collision, below $\epsilon = 1$ GeV fm^{-3}, by using the most peripheral (not yet investigated) Pb + Pb collisions or collisions of lighter nuclei at the highest beam energy at SPS ($\sqrt{s} = 17$, 19 GeV).

Another piece of information important for the understanding of charm production in nuclear collisions would be the direct comparison of the $(J/\Psi)/DY$ and the $(J/\Psi)/D\overline{D}$ ratios in nuclear collisions at $\sqrt{s} < 19$ GeV and in p + $\overline{\text{p}}$ collisions at the Tevatron. Tevatron reaches an energy density similar to or larger than the one estimated in very central S + S collisions at 200 A GeV [48]. Therefore it would supply a comparison for these points and a continuation of the absorption line fitted through the p + p and p + A data measured by NA50 (figure 6), or otherwise. Differences due to the change of dominant production mechanisms of charm in p + $\overline{\text{p}}$ collisions as compared to A + B and p + p can be accounted for theoretically. A high E_T cut could additionally help in sorting out 'central' p + $\overline{\text{p}}$ collisions. This comparison should be done possibly in the very same dimuon mass region for all processes (also DY), e.g. using Monte Carlo's tuned to p + $\overline{\text{p}}$ Tevatron data.

This comparison would answer the question whether the energy density is indeed the only critical variable for the appearance of a thermalized QGP state with three effective flavours u, d, s, or whether there is also a critical volume (e.g. as measured by the L variable: $V \sim L^3$). Furthermore, at present the comparison of nuclear collisions to p+p and p+A data is done at the same energy and not at the same energy density. This issue is important, since if for example the energy density is the only critical scale variable, the QGP should be formed also in elementary collisions like p + $\overline{\text{p}}$ at a higher beam energy and the same energy density.

Further it is important to search for thresholds in the production of many particles, e.g. Ω, which was found to be enhanced by a factor 15 above p + A data in Pb + Pb collisions at

158 A GeV [49] in the energy density region corresponding to the green stars in figure 9(b). Similarly interesting would be a measurement of the invariant mass of e^+e^- in low energy densities.

6. Conclusions

In this paper, consequences resulting from the viable possibility that the dimuon invariant mass ($m(\mu^+\mu^-)$) enhancement, measured by the NA50 experiment in the IMR between the ϕ and the J/Ψ mass, in S + U and Pb + Pb collisions at $\sqrt{s} = 19$, 17 GeV, reflects a $D\overline{D}$ enhancement over expectations are worked out.

The dependence of the J/Ψ and the $D\overline{D}$ yields per collision in Pb + Pb collisions on the mean number of participants has been estimated. This dependence reveals the non-thermal features of charm production at this energy. The $\sim N_p^{0.7}$ dependence of the J/Ψ yield (figure 3) suggests stronger dissociation of J/Ψ with higher centrality. The dissociation is stronger than the absorption seen in any other hadron, e.g. $\overline{\mathrm{p}}$ in Pb + Pb collisions. The N_p dependence of the $D\overline{D}$ yield of $N_p^{1.7}$ (figure 2) also indicates non-thermal open charm production at this energy, showing up in an excess rather than reduction as compared to the thermal expectation.

If the dimuon excess observed by NA50 is due to open charm, and even otherwise, it is appropriate to search for an anomalous suppression of J/Ψ as compared to the total open charm production, rather than to the DY process. We therefore investigated here the $(J/\Psi)/D\overline{D}$ ratio in Pb + Pb collisions and we found that it decreases approximately as $\sim N_p^{-1}$ (figures 4 and 5).

Note that if the J/Ψ were completely dissociated in quark gluon matter and were later dominantly formed through $c\bar{c}$ quark coalescence, we would expect that $(J/\Psi)/D\overline{D}$ is $\sim N_p^{-1}$, as actually seen†. In that case, based on coalescence arguments, the $(J/\Psi)/D\overline{D}$ ratio could be used to estimate the volume of the charm source, which may reflect the size of the quark gluon plasma. This is probable under the assumption that the final measured J/Ψ is dominated by the J/Ψ originating from $c\bar{c}$ pairs which travel through the plasma volume, an assumption which may hold only for large plasma volumes, i.e. for the most central collisions.

We give an estimate of the volume of the charm source for the most central Pb + Pb collisions assuming a coalescence Ansatz. The volume of the charm source is estimated to be $V_{charm\ source} \sim 64.6$ fm^3, and assuming a sphere the radius $R_{charm\ source}$ is 2.49 fm. The latter value is similar to the expectation of $\sim$2.43 fm for the charm source radius at the thermal freeze-out, if the m_T dependence of the radius is taken into account.

A further consequence of a possible open charm enhancement is that the J/Ψ over the $D\overline{D}$ ratio appears to be suppressed already in S+U collisions as compared to p+A collisions, unlike the $(J/\Psi)/DY$ ratio (figure 6). The $\psi'/D\overline{D}$ ratio would also be additionally suppressed as compared to the ψ'/DY in both S + U and Pb + Pb collisions. These phenomena could be interpreted as the onset of dissociation of bound charm states above the energy density $\epsilon \sim 1$ GeV fm^{-3}.

We have estimated and compared the dependence of the $(J/\Psi)/D\overline{D}$ ratio and of the kaon multiplicity per volume in several collisions and $\sqrt{s}$ as a function of the initial energy density. We find that both the kaon number density and the ratio $(J/\Psi)/D\overline{D}$ exhibit dramatic changes

† We assumed that N_p is proportional to the volume of the $c\bar{c}$ source and the charm quark multiplicity is approximately one, in the events in which charm particles are produced.

at the energy density of 1 GeV fm^{-3}, as demonstrated in figure 9. This is the main result of this paper.

It follows that three major QGP signatures ($s\bar{s}$ enhancement, ρ changes and J/Ψ suppression) all appear above the energy density of $\sim$1 GeV fm^{-3}, which is the critical energy density for the QGP phase transition according to lattice QCD.

This discussion underlines the importance of a direct measurement of open charm production in nuclear collisions, and of other experimental investigations proposed in section 5, for the understanding of ultrarelativistic nuclear reactions and the dynamics of the QGP phase transition.

Acknowledgments

I would like to thank Professors P Minkowski, K Pretzl, U Heinz and J Rafelski for stimulating discussions, and Doctors C Cicalo, O Drapier, C Gerschel, E Scomparin, P Seyboth, F Sikler, P Sonderegger, M Tannenbaum, U Wiedemann, and especially J Y Ollitrault for clarifying discussions on their data and/or for communicating their results to me. We thank the Swiss National Science Foundation for their support.

Note added in proof. In the time since the preprint of the present paper has been completed (SLAC preprint server hep-ph/0004138), a second possible interpretation of figure 7(b) was realized in [51] and followed in [52]. A discussion of strangeness production as QGP signature can be found in [53].

The dependence of charm in nucleus + nucleus collisions on the number of participant nucleons, the production of charm through coalescence mechanisms and other features of charm production in ultrarelativistic nucleus + nucleus collisions are discussed in many recent papers, for example [55]–[60].

References

[1] Laermann E 1996 *Nucl. Phys.* A **610** 1c
[2] Schäfer T 1996 *Nucl. Phys.* A **610** 13c
[3] Bass S A *et al* 1999 *J. Phys. G: Nucl. Part. Phys.* **25** R1–57
(Bass S A *et al* 1998 *Preprint* hep-ph/9810281)
Stock R 1999 *Nucl. Phys.* A **661** 282c
Müller B 1999 *Nucl. Phys.* A **661** 272c
[4] Matsui T and Satz H 1986 *Phys. Lett.* B **178** 416
[5] Abreu M C *et al* (NA50 Collaboration) 2000 *Phys. Lett.* B **477** 28–36
(Abreu M C *et al* (NA50 Collaboration) 2000 *Preprint* CERN-EP-2000-013)
[6] Abreu M C *et al* (NA50 Collaboration) 2000 *Eur. Phys. J.* C **14** 443–55
(Abreu M C *et al* (NA50 Collaboration) 2000 *Preprint* CERN-EP-2000-012)
[7] Lin Z *et al* 1998 *Phys. Lett.* B **444** 245
[8] Soave C 1998 *PhD Thesis* Universita Degli Studi Di Torino, Italy
[9] Rapp R and Shuryak E 2000 *Phys. Lett.* B **473** 13–19
(Rapp R and Shuryak E 1999 *Preprint* hep-ph/9909348)
Gallmeister K *et al* 2000 *Phys. Lett.* B **473** 20–24
(Gallmeister K *et al* 1999 *Preprint* hep-ph/9908269)
Huovinen P *et al* 1999 *Nucl. Phys.* A **650** 227
[10] Minkowski P 1979 *Phys. Lett.* B **85** 231
Halzen F *et al* 1983 *Phys. Rev.* D **27** 1631
Brodsky S *et al* 1981 *Phys. Rev.* D **23** 2745

[11] Abreu M C *et al* (NA50 Collaboration) 1999 *Phys. Lett.* B **450** 456
[12] Gerschel C 1999 Private communication
[13] Ollitrault J Y 1999 Private communication
[14] Blaizot J P and Ollitrault J Y 1996 *Phys. Rev. Lett.* **77** 170
[15] Ambrosini G *et al* (NA52 Collaboration) 1999 *New J. Phys.* **1** 22
[16] Ambrosini G *et al* (NA52 Collaboration) 1999 *New J. Phys.* **1** 23
(Ambrosini G *et al* (NA52 Collaboration) 1999 *Preprint* CERN-OPEN-99-313)
Kabana S *et al* (NA52 Collaboration) 2001 *J. Phys. G: Nucl. Part. Phys.* **27** 495
(Kabana S *et al* (NA52 Collaboration) 2000 *Preprint* hep-ex/0010053)
Kabana S *et al* (NA52 Collaboration) 2000 *ICHEP2000* submitted
(Kabana S *et al* (NA52 Collaboration) 2000 *Preprint* hep-ph/0010045)
Kabana S *et al* (NA52 Collaboration) 1998 *Nucl. Phys.* A **638** 411c
Kabana S *et al* (NA52 Collaboration) 1997 *J. Phys. G: Nucl. Part. Phys.* **23** 2135
[17] Gerschel C 1999 *Lectures given in the Cracow School of Theoretical Physics, XXXIX Course* IPNO-DR 99-33
[18] Fleuret F 1997 *PhD Thesis* Ecole Polytechnique, France
[19] Abreu M C *et al* (NA50 Collaboration) 1997 *Phys. Lett.* B **410** 337
[20] Sonderegger P 1999 Private communication
[21] Abreu M *et al* (NA50 Collaboration) 2000 *Eur. Phys. J.* C **13** 69
(Abreu M *et al* (NA50 Collaboration) 1999 *Preprint* CERN-EP/99-112)
[22] Abreu M *et al* (NA51 Collaboration) 1998 *Phys. Lett.* B **438** 35
Lourenco C 1996 *Nucl. Phys.* A **610** 552
(Lourenco C 1996 *Preprint* CERN-PPE-96-158)
[23] Buchmüller W and Tye S 1981 *Conf. on Perturbative Quantum Chromodynamics (25–28 March 1981, FL)* FERMILAB-Conf-81/38-THY
[24] Heinz U and Wiedemann U 1999 *Phys. Rep.* **319** 145–230
Ferenc D *et al* 1999 *Phys. Lett.* B **457** 347–52
Heinz U and Jacak B 1999 *Ann. Rev. Nucl. Sci.* **49** 529
[25] Albini *et al* 1975 *Nucl. Phys.* B **84** 269
[26] Ganz R (NA49 Collaboration) 1999 *Nucl. Phys.* A **661** 448c
[27] Wiedemann U 1999 *Nucl. Phys.* A **661** 65c
[28] Cleymans J and Redlich K 1999 *Phys. Rev.* C **60** 054 908
[29] Kolb E and Turner M 1990 *The Early Universe* (New York: Addison-Wesley)
[30] Soltz R A (E866 Collaboration) 1999 *Nucl. Phys.* A **661** 439c
[31] Ahle L *et al* (E802 and E866 Collaborations) 1999 *Phys. Rev.* C **60** 044 904
(Ahle L *et al* (E802 and E866 Collaborations) 1999 *Preprint* nucl-ex/9903009)
[32] Sikler F *et al* (NA49 Collaboration) 1999 *Nucl. Phys.* A **661** 45c
[33] Seyboth P (NA49 Collaboration) 1999 *Talk Given in CERN Heavy Ion Forum (26 July 1999)*
[34] Andersen E *et al* (WA97 Collaboration) 1999 *Phys. Lett.* B **449** 401
(Andersen E *et al* (WA97 Collaboration) 1999 *Preprint* CERN-EP-99-029)
[35] Bjorken J D 1983 *Phys. Rev.* D **27** 140
[36] Braun-Munzinger P and Stachel J 1998 *Nucl. Phys.* A **638** 3
(Braun-Munzinger P and Stachel J 1998 *Preprint* nucl-ex/9803015)
[37] Margetis S *et al* (NA49 Collaboration) 1995 *Phys. Rev. Lett.* **75** 3814
[38] Bächler J *et al* (NA35 Collaboration) 1991 *Z. Phys.* C **51** 157
[39] Werner K 1993 *Phys. Rep.* **232** 87
[40] Kabana S *et al* (NA52 Collaboration) 1999 *J. Phys. G: Nucl. Part. Phys.* **25** 217
[41] Kabana S *et al* (NA52 Collaboration) 1999 *Nucl. Phys.* A **661** 370c
[42] Koch P, Müller B and Rafelski J 1986 *Phys. Rep.* **142** 167
[43] Satz H 1999 *Nucl. Phys.* A **661** 104c

[44] Lenkeit B *et al* 1999 (CERES Collaboration) *Nucl. Phys.* A **661** 23c
[45] Rapp R 1999 *Nucl. Phys.* A **661** 33c
[46] Kabana S and Minkowski P 2000 *Phys. Lett.* B **472** 155
(Kabana S and Minkowski P 1999 *Preprint* hep-ph/9907570)
Minkowski P *et al* 2000 *Preprint* hep-ph/0011040
Kabana S and Minkowski P 1999 *Proc. Conf. HEP99 (Tampere, Finland, 1999)* p 862
(Kabana S and Minkowski P 1999 *Preprint* hep-ph/9909351)
[47] Cicalo C *et al* 1999 *Letter of Intent* CERN/SPSC 99-15; SPSC/I221; 7 May
[48] Bartke J *et al* 1990 *Z. Phys.* C **48** 191
[49] Andersen E *et al* 1999 (WA97 Collaboration) *Phys. Lett.* B **449** 401
[50] Ahle L *et al* (E802 Collaboration) 1994 *Phys. Lett.* B **332** 258
Tannenbaum M 1999 Private communication
[51] Kabana S 2001 *J. Phys. G: Nucl. Part. Phys.* **27** 497
(Kabana S 2000 *Preprint* hep-ph/0010228)
Kabana S 2001 *Proc. ICHEP2000* to appear
(Kabana S 2000 *Preprint* hep-ph/0010246)
[52] Kabana S and Minkowski P 2001 *New J. Phys.* **3** 4
(Kabana S and Minkowski P 2000 *Preprint* hep-ph/0010247)
[53] Kabana S 2001 *Eur. Phys. J.* C to appear
(Kabana S 2001 *University of Bern Preprint* BUHE-2001/01, hep-ph/0104001)
[54] Brodsky S and Mueller A 1988 *Phys. Lett.* B **206** 685
(Brodsky S and Mueller A 1988 *Preprint* SLAC-PUB-4015)
[55] Braun-Munzinger P and Stachel J 2000 *Phys. Lett.* B **490** 196
(Braun-Munzinger P and Stachel J 2000 *Preprint* nucl-th/0007059)
[56] Levai P *et al* 2000 *Preprint* hep-ph/0007247
Levai P *et al* 2000 *Preprint* nucl-th/0011023
Levai P *et al* 2000 *Preprint* hep-ph/0008195
[57] Cassing W *et al* 2000 *Preprint* nucl-th/0010071
[58] Gorenstein M, Kostyak A, Stocker H and Greiner W 2000 *Preprint* hep-ph/0012015
Gorenstein M *et al* 2000 *Preprint* hep-ph/0010148
Schmitt J *et al* 2000 *Preprint* hep-ph/0009258
[59] Satz H 2000 *Rep. Prog. Phys.* **63** 1511
Gazdzicki M 2000 *Preprint* hep-ph/0009221
[60] Thews R, Schroedter M and Rafelski J 2000 *Preprint* hep-ph/0007323
Hufner J, Kopeliovich B and Polleri A 2000 *Preprint* hep-ph/0010282
Patra K and Srivastava D 2000 *Preprint* hep-ph/0009097
Blaizot J P and Ollitrault J Y 2000 *Preprint* nucl-th/0007020
Zhang B *et al* 2000 *Preprint* nucl-th/0007003
Blaschke D *et al* 2000 *Preprint* nucl-th/0006071